Resistive signature of excitonic coupling in an electron-hole double layer with a middle barrier

Xingjun Wu, Wenkai Lou, Kai Chang, Gerard Sullivan, and Rui-Rui Du

Resistive Signature of Excitonic Coupling
in Electron-Hole Double Layer with a Middle Barrier

Xingjun Wu,[1,*] Wenkai Lou,[2] Kai Chang,[2]

Gerard Sullivan,[3] and Rui-Rui Du[1,4,*]

[1]*International Center for Quantum Materials, School of Physics, Peking University,*

Beijing 100871, China

[2] *SKLSM, Institute of Semiconductors, Chinese Academy of Sciences, Beijing 100083, China*

[3] *Teledyne Scientific and Imaging, Thousand Oaks, California 91603, USA*

[4] *Department of Physics and Astronomy, Rice University, Houston, Texas 77251-1892, USA*

*Email address: wxj_icqm@pku.edu.cn

rrd@rice.edu

ABSTRACT

We study the interlayer scattering mediated by long-range Coulomb interaction between electrons (density n) and holes (p) in a double-layer system. The gated device is made of InAs (e) and InGaSb (h) quantum wells separated by a AlSb middle barrier such that the interlayer tunneling is negligibly small. By using independent-layer contacts we measure the transport tensor ρ_{xx} and ρ_{xy} that are solely from the InAs layer, while sweeping p in the InGaSb layer. We found a strongly enhanced resistive scattering signal as the carrier densities approach a total charge neutrality, $n = p$, which cannot be described by the Fermi liquid theory. Results of data analysis for density, temperature, and magnetic field dependences are consistent with the emergence of excitonic coupling between the two layers, stressing the dominance of Coulomb interaction even in the presence of disorder.

Key words: double layer, exciton, interlayer correlation, *e-h* Coulomb interaction

Introduction- Interlayer interaction in closely spaced two-dimensional (2D) systems can produce a wealth of exotic phenomena with no counterpart in the single-layer case [1-10]. For example, even denominator fractional quantum Hall states (FQHS) at the total filling factors $\upsilon = 1/4$ and 1/2 are discovered in high mobility GaAs double-layer or wide quantum-well (QW) structures [1-4]; conversely, quantum Hall states at selected-integer filling factors in double-quantum-well (DQW) structures are found missing in high-magnetic-field regime [5,6]; and a pinned bilayer quantum Wigner crystal is observed originating from the intralayer and interlayer interactions [7]. Excitonic interaction in double-layer systems, as one of the most interesting examples of interlayer interactions, has produced a large number of many-body phenomena. Exciton condensation in quantum Hall (QH) bilayer GaAs system at total filling factor $\upsilon = 1$ [8-14] has been well studied and recently extended to graphene double layers [15,16]. Enhanced resonant interlayer tunneling [8], dissipation-less counter-flow transport [9-12] and perfect Coulomb drag signals [14,15] are the manifestations of interlayer excitonic correlation. Moreover, in coupled electron-hole double layers, an electron confined in one layer may bind with a hole in the other layer, spontaneously forming excitonic states in zero magnetic field [8-16]. The possibility of realizing exciton condensation in such a novel setting has been discussed in a large number of theoretical works [17-25]. The recent observation of strongly enhanced tunneling at total charge neutrality in double-bilayer graphene-WSe_2 shows encouraging progress in realizing the spontaneous exciton condensate in zero magnetic field [26].

Due to a unique inverted band structure with a finite overlap of the InAs conduction band and GaSb valence band, electrons and holes could coexist in InAs/GaSb QWs, but partially confined in respective InAs or GaSb QW. Spontaneous formation of an excitonic ground state in zero magnetic field in this material system has been proposed in Ref. [20,21]. Recently, the evidences for a BCS-like gap were observed in both THz transmission and electrical transport

measurements, in an inverted, dilute InAs/GaSb system [27], consistent with a topological excitonic insulator. In this paper, we investigate an electron-hole double-layer with a middle barrier, in which electrons and holes of individual layer are decoupled electrically. In such structure the evidence for excitonic coupling by Coulomb interaction can be studied without concerning the role of interlayer tunneling.

Devices and measurements- The sample used in our experiment was grown by molecular beam epitaxy (MBE) on (100) InAs substrate, consisting of 9.5nm InAs and 5nm $In_{0.25}Ga_{0.75}Sb$ layers separated by a 10nm-thickness AlSb middle barrier. Here the GaSb layer is replaced by a ternary compound $In_{0.25}Ga_{0.75}Sb$, which is about 1 % compressive strain [28]. As a result the hole carriers should acquire a reduced mass in the plane, making a better match with the electron mass in InAs. The DQW structure is encapsulated between two AlGaSb barrier layers. The sample was wet etched into a standard Hall bar of 20μm by 40μm size. Ohmic contacts for connecting electron layer were made by etching selectively down to the InAs QW and depositing Ti/Ni/Au without annealing, while Ohmic contact for connecting both layers was made by depositing Indium with annealing. Dual gates were fabricated on both sides with aluminum. While the InAs substrate is conductive at low temperature and can serve as a global bottom gate, often it is desirable to make a local gate. To this end we adopt the "flip-chip" process [29] where the front side of the structure is bond to a supporting GaAs substrate, and the InAs substrate is then selectively etched, leaving a ~0.2μm thick DQW and the buffer layer. A metallic layer is subsequently deposited onto the buffer layer surface and being patterned lithographically into a local bottom gate (Fig. 1(a)). Details can be found in supplemental materials.

The electron (hole) density at zero gate bias is $11 \times 10^{11} cm^{-2}$ ($7 \times 10^{11} cm^{-2}$), the

low temperature (~0.3K) mobility of electron layer is ~ 10 m^2 V^{-1}s^{-1}, hole layer shows a lower mobility of ~ 1 m^2 V^{-1}s^{-1} partly due to strain. Overall either the electron or hole mobility is lower than those of InAs/GaSb, attributing to the increasing scattering from interface roughness with AlSb, and to the fact that AlSb is susceptible to oxidation during processing. As a result, the present samples should be in the weakly disordered regime as far as single-electron transport is concerned. Nevertheless, as we shall elaborate throughout the paper, the Coulomb interactions are still dominating over the disorder effect, such as Anderson localization, in our electron-hole double-layers.

Fig. 1(c) shows the schematic view of our measurements. The bottom hole layer was gated by a voltage V$_{BG}$, while the top electron layer was gated by a voltage V$_{TG}$. Two layers were connected with each other through a common grounding point. In this measurement, we applied a small alternating current (~100nA) into the higher mobility InAs layer and studied this top layer using a low frequency lock-in setup through measuring longitudinal and Hall resistivities, ρ$_{xx}$ and ρ$_{xy}$. By measuring ρ$_{xy}$ in magneto-transport, we can easily determine *n* in the top layer. In this configuration, we keep a series of nearly constant hole densities *p* in the bottom layer with V$_{BG}$ and sweep V$_{TG}$ to vary *n* in the top layer. Ideally, due to the effective screening of the inserted hole layer, V$_{BG}$ would not vary *n* in the top layer unless *p* in the bottom layer is extremely low. Otherwise, the electron-layer longitudinal resistivity ρ$_{xx}$ in this configuration can be derived phenomenologically from the Drude-like formula [30]:

$$\rho_{xx} = \frac{m_1}{e^2 n_1}\left(\frac{1}{\tau} + \frac{1}{\tau_D}\right) \qquad (1)$$

Where m_1 and n_1 are the electron effective mass and density in the top layer, τ^{-1} and τ_D^{-1}

are the scattering rates from intralayer and interlayer contributions. Due to the effective screening of the hole layer, V_{BG} would not change the intralayer scattering rate τ^{-1} in the top layer. So the V_{BG}-dependent ρ_{xx} is a good approach to study the interlayer scattering rate τ_D^{-1} analogous to the drag resistivity of Coulomb drag measurement [31]. Due to the technical problem of making an independent hole contact [32] in the system, Coulomb drag measurement seems to be difficult. In spite of this, the current measurement circuit, in fact, presents the effect of Coulomb drag between the two layers in terms of interlayer scattering, where the hole layer is in an open-circuit.

Fig. 1(b) shows the corresponding result of eight-band $k\cdot p$ calculation. It has been known that the interlayer tunneling in InAs/GaSb DQWs would lead to a hybridization gap opening at the crossing points between the electron and hole dispersion relations [33]. While by inserting a 10nm-thickness AlSb barrier, we can find the tunneling-induced hybridization gap cannot be resolved in our numerical calculations, consistent with the previous experiment reports [34,35](*i.e.* the critical AlSb thickness for a two-independent-layer system is 2nm). Experimentally, by independently contacting the InAs layer, the single-layer characteristics have been observed in magneto-transport measurements (see supplemental materials). The interlayer tunneling resistance values are estimated on the order of at least tens of megaohms. The single-layer resistance measurement errors associated with finite interlayer resistance shown in this letter are on the order of less than 1%.

Figure 2 shows the gate-voltage dependent ρ_{xx} and n in the InAs layer. Here n is determined from the low-field slope of Hall resistances and V_{BG} is chosen at certain voltage values where we'll see later the holes screen effectively to the back gate potential. Hole

densities p at V_{BG}=2.5V, 5V, 7.5V in the figure correspond to 4.9, 2.4, $0.4\pm0.1 \times 10^{11} cm^{-2}$

respectively, which is determined from a two-layer-connected sample of the same wafer.

From the top panel in Fig. 2, it can be found that, ρ_{xx} increases rapidly first as the electrons

in the top layer is being depopulated. When V_{TG} exceeds -1.6V, the increasing rate of ρ_{xx}

becomes much slower. The top gate could not tune the electron Fermi level effectively any

more. Meanwhile, we observe the gate hysteresis of ρ_{xx} on opposite-directed sweeps of V_{TG}

(not shown). It is likely to be caused by some disorder-induced charge donor states around

this energy level, *e.g.*, due to the surface donors [36], deep donors in AlSb [37] or interface

donor states at InAs/AlSb [38]. Such donor states would trap and donate electrons in response

to the increase and decrease of V_{TG}, which impedes V_{TG} to tune the Fermi level effectively.

By applying a more positive V_{BG}, we find ρ_{xx} increases further and n in the top layer could

be tuned lower. This could be due to the band bending caused by increasing V_{BG}. By

increasing perpendicular electric field across the sample, the band bending in the InAs

electron well (which is relatively wide) would result in an upward shift of the conduction

band edge at the center of the InAs well, relative to the donor levels like those at the

InAs/AlSb interface. Thus the electron density could be tuned lower simply owning to a

reduction of donor states above the electron Fermi level. We would also expect an obvious

change in the electron density when the electron chemical potential in InAs is tuned to cross

the center of the energy levels of the donor states, which is observed around V_{BG} =6V in Fig.

3(b).

Enhanced interlayer scattering around charge neutrality in zero magnetic field- In order to

analysis the interlayer Coulomb interaction further, we map the longitudinal resistivity ρ_{xx}

symmetrically as a function of V_{TG} and V_{BG} at $B = 0T$, as shown in Fig. 3(a). The three cases

of V_{TG} = -1.98V, -1.72V, -1V are extracted and plotted in Fig. 3(b), 3(c), 3(d), respectively.

From Fig. 3(d), it can be found that, due to the effective screening of the hole layer, n keeps a

nearly constant value of $4.8 \times 10^{11} cm^{-2}$ on sweeps of V_{BG} (V_{BG} < 8V) and ρ_{xx} remains

invariant as well. When V_{BG} exceeds 8V, p in the bottom layer has become very low, it can

only screen a fraction of the electro-static potential from V_{BG}, resulting in n in the top layer

increasing and ρ_{xx} following to decrease. The partial screening effect can also be found in

Fig. 3(b) and 3(c). As V_{TG} is applied more negatively, the Fermi level moves downward into

an energy range occupied by charge donor states, then is nearly pinned around this energy

level (this level is located around n =$1.5 \times 10^{11} cm^{-2}$, seen from Fig. 3). By increasing the

perpendicular electric field with a more positive V_{BG}, the band bending in the InAs well

would result in a relative shift between the conduction band edge at the center of the InAs

well and the donor levels like those at the InAs/AlSb interface, and thus n could be tuned

lower as discussed in Fig. 2.

The most interesting observation is that the ρ_{xx} dramatically displays a strongly

enhanced signal on sweeps of V_{BG} in the regime of V_{TG} < -1.7V (n <$1.2 \times 10^{11} cm^{-2}$) as

shown in Fig. 3(a). When V_{TG} = -1.98V, the signal increases by almost 50% and is localized

around total charge neutrality ($n \sim p = 0.8 \pm 0.15 \times 10^{11} cm^{-2}$). This is our main finding what

we will discuss below. According to equation (1), ρ_{xx} depends on two relevant parameters

-electron density n and low-temperature total scattering rate τ_t^{-1}. It can be seen clearly from

Fig. 3(b), the evolution of ρ_{xx} roughly follows n except around the signal position, where n

continues to vary smoothly. The rapid raise of ρ_{xx}, or equivalently, a sudden jump of the

scattering rate around total charge neutrality, is strongly suggestive for the formation of excitonic coupling between the two layers. The Fermi-liquid theory dealing with interlayer scattering seems to be invalid in this case [30]. In Fermi-liquid theory, interlayer Coulomb interaction is usually assumed to be weak, the transport properties of each layer are often expected to be dominated by disorder, *i.e.*, $\tau \ll \tau_D$. These assumptions apply to most cases. However, our observation seems to be less trivial because if that is the case ρ_{xx} in Eq. (1) is supposed to be difficult to reflect interlayer Coulomb scattering. To be specific, Fermi-liquid result is obtained under this assumption: $\ell \ll d$ [30], where ℓ is the electron mean-free path and d is the interlayer separation. In our case, ℓ at V_{TG} = -1.98V can be derived quantitatively by fitting Eq. (1), $\ell = 15$nm(see supplemental materials), comparable to d = 10nm, which motivates us to think about other scattering mechanisms. Another possible explanation is based on the phonon-mediated interaction, and this can be ruled out by temperature dependence (shown in Fig.4). Interlayer scattering assisted by phonon is expected to be enhanced as T increases, contradiction with our observation that the scattering signal is submerged with T increasing.

It is illustrative to consider the inter-particle distance r_d in the top layer around the peak position, $r_d = n^{-1/2}$ =35nm at V_{TG} = -1.98V, which is larger than interlayer distance (d =10nm). Excitonic coupling between two layers make it possible to form a collective state like quantum Hall bilayer state [13]. As the concentration of per carrier type decreases, interlayer excitonic correlation is expected to increase due to the reduced screening. It can account for the exacerbated interlayer scattering signal with lower n in Fig. 3.

Discussion of the origins of the strongly enhanced scattering signal- To gain further insight

into the origin of the enhanced scattering signal around $n \sim p$, magnetic-field and temperature dependences are measured. Fig. 4(a) shows the temperature dependence. We can find a decreasing resistivity background with T increasing. This could be due to more donor states becoming active to release electrons to participate in the conductivity at higher T [39]. In addition to the decreasing resistivity background, it is interesting to find that, the resistivity signal becomes weakened as T increases, and finally is submerged by the background around 15~19K. This observation contradicts with Coulomb scattering phase-space argument [30], that is, increasing T will increase scattering phase space, thus an increasing resistivity is expected. It implies a character of an insulating state instead. This insulating state characterized by one layer is difficult to understand in term of a picture of two-uncorrelated-layer structure. We explain this unusual insulating state as a collective behavior of double-layer system probably due to the opening of an interlayer exciton-like gap.

Parallel magnetic field dependent ρ_{xx} also has been presented in Fig. 4(b). It can rule out the possibility that this collective insulator state arises from an interlayer tunneling-induced gap. With applying $B_{//}$, the electron and hole dispersion relations would induce a relative shift proportional to their relative displacement in real space Δz. The regions where exist electron-hole band mixing are expected to move away from the Fermi energy and thus the resistivity would decrease with increasing $B_{//}$ [40]. It is opposite to our observation. One possible explanation is that a virtual transition between electron and hole bands would be attenuated with increasing $B_{//}$, immune to an increased dielectric constant, hence lowered exciton binding energy. Thus, the resistivity signal is expected to be

strengthened with increasing $B_{//}$ as shown in Fig. 4(b). We further examine the perpendicular magnetic field dependent ρ_{xx} at V_{TG} = -1.98V as shown in Fig. 4(c). Interestingly, we find the signal shows a significant $B_\perp$ dependence, where a $\sim B^2$ dependence is observed as shown in the inset. An enlarged scattering phase space due to the increase of Landau level degeneracy at higher fields cannot explain the strong field dependence. In the assumption of a constant interlayer perturbation, the scattering rate based on Fermi's golden rule is expected to grow linearly with $B_\perp$, slower than the quadratic dependence, indicating a $B_\perp$-promoted interlayer interaction. This is consistent with the prediction of interlayer exciton-like interaction. $B_\perp$ is expected to enhance the confinement, hence, the binding energy.

In conclusion, we have measured longitudinal- and Hall signals of InAs layer in the presence of a spatially close InGaSb layer. We observed a strongly enhanced interlayer scattering around charge neutrality. Results of data analysis for density, temperature, and magnetic field dependences are consistent with the emergence of excitonic coupling between the two layers, stressing the dominance of Coulomb interaction even in the presence of disorder.

References

1. D. R. Luhman, W. Pan, D. C. Tsui, L. N. Pfeiffer, K. W. Baldwin, and K. W. West. Observation of a fractional quantum Hall state at v =1/4 in a wide GaAs quantum well. *Phys. Rev. Lett.* **101**, 266804 (2008).

2. J. Shabani, T. Gokmen, Y. T. Chiu, and M. Shayegan. Evidence for developing fractional quantum Hall states at even denominator 1/2 and 1/4 fillings in asymmetric wide quantum wells. *Phys. Rev. Lett.* **103**, 256802 (2009).

3. J. P. Eisenstein, G. S. Boebinger, L. N. Pfeiffer, K. W. West, and Song He. New fractional quantum Hall state in double-layer two-dimensional electron systems. *Phys. Rev. Lett.* **68**, 1383 (1992).

4. Y. W. Suen, L. W. Engel, M. B. Santos, M. Shayegan, and D. C. Tsui. Observation of a v=1/2 fractional quantum Hall state in a double-layer electron system. *Phys. Rev. Lett.* **68**, 1379 (1992).

5. G. S. Boebinger, H. W. Jiang, L. N. Pfeiffer, and K. W. West. Magnetic-field-driven destruction of quantum Hall states in a double quantum well. *Phys. Rev. Lett.* **64**, 1793 (1990).

6. A. H. MacDonald, P. M. Platzman, and G. S. Boebinger. Collapse of integer Hall gaps in a double-quantum-well system. *Phys. Rev. Lett.* **65**, 775 (1990).

7. H. C. Manoharan, Y. W. Suen, M. B. Santos, and M. Shayegan, Evidence for a bilayer quantum Wigner solid. *Phys. Rev. Lett.* **77**, 1813 (1996).

8. I. B. Spielman, J. P. Eisenstein, L. N. Pfeiffer, and K. W. West. Resonantly enhanced tunneling in a double layer quantum Hall ferromagnet. *Phys. Rev. Lett.* **84**, 5808 (2000).

9. Y. Yoon, L. Tiemann, S. Schmult, W. Dietsche, K. von Klitzing, and W. Wegscheider. Interlayer tunneling in counterflow experiments on the excitonic condensate in quantum Hall bilayers. *Phys. Rev. Lett.* **104**, 116802 (2010).

10. E. Tutuc, M. Shayegan, and D. A. Huse. Counterflow measurements in strongly correlated GaAs hole bilayers: evidence for electron-hole pairing. *Phys. Rev. Lett.* **93**, 036802 (2004).

11. M. Kellogg, J. P. Eisenstein, L. N. Pfeiffer, and K. W. West. Vanishing Hall resistance at high magnetic field in a double-layer two-dimensional electron system. *Phys. Rev. Lett.* **93**, 036801 (2004).

12. R. D. Wiersma, J. G. S. Lok, S. Kraus, W. Dietsche, K. von Klitzing, D. Schuh, M. Bichler, H. P. Tranitz, and W. Wefscheider. Activated transport in the separate layers that form the ν_t =1 exciton condensate. *Phys. Rev. Lett.* **93**, 266805 (2004).

13. J. P. Eisenstein and A. H. MacDonald. Bose-Einstein condensation of excitons in bilayer electron systems. *Nature* **432**, 691 (2004).

14. D. Nandi, A. D. K. Finck, J. P. Eisenstein, L. N. Pfeiffer, and K. W. West, Exciton condensation and perfect Coulomb drag, *Nature*, **488**, 481 (2012).

15. Xiaomeng Liu, K. Watanabe, T. Taniguchi, Bertrand I. Halperin, and Philip Kim. Quantum Hall drag of exciton condensate in graphene. *Nat. Phys.* **13**, 746 (2017).

16. J. I. A. Li, T. Taniguchi, K. Watanabe, J. Hone, and C. R. Dean. Excitonic superfluid phase in double bilayer graphene, *Nat. Phys.* **13**, 751 (2017).

17. Yu. E. Lozovik and Y. I. Yudson, Feasibility of superfluidity of paired spatially separated electrons and holes; a new superconductivity mechanism. *Sov. Phys. JETP Lett.* **22**, 274

(1975).

18. C. Comte, P. Nozières, Exciton Bose condensation: the ground state of an electron-hole gas – I. Mean field description of a simplified model. *J. Phys*. **43**, 1069 (1982)

19. X. Zhu, P. B. Littlewood, M. S. Hybertsen, and T. M. Rice, Exciton condensate in semiconductor quantum well structures. *Phys. Rev. Lett.* **74**, 1633 (1995)

20. Y. Naveh, and B. Laikhtman, Excitonic instability and electric-field-induced phase transition towards a two-dimensional exciton condensate. *Phys. Rev. Lett*. **77**, 900 (1996).

21. S. Datta, M. R. Melloch, and R. L. Gunshor, Possibility of an excitonic ground state in quantum wells. *Phys. Rev. B* **32**, 2607(1985).

22. Mott, N. F. The transition to the metallic state. *Phil. Mag.* **6**, 287 (1961).

23. Knox, R.S. Theory of excitons. *Solid State Phys. Suppl*. **5**, 100 (1963).

24. Keldysh, L. V. and Kopaev, Y. V. Possible instability of the semimetallic state toward coulomb interaction. *Fiz. Tverd. Tela* **6**, 2791(1964).

25. Jérome, D., Rice, T. M. & Kohn, W. Excitonic insulator. *Phys. Rev.* **158**, 462 (1967).

26. G. William Burg, Nitin Prasad, Kyounghwan Kim, Takashi Taniguchi, Kenji Watanabe, A. H. MacDonald, L. F. Register, and E. Tutuc. Strongly enhanced tunneling at total charge neutrality in double-bilayer graphene-WSe$_2$ heterostructures. *Phys. Rev. Lett.* **120**, 177702 (2018).

27. L. J. Du, X. Li, W. Lou, G. Sullivan, K. Chang, J. Kono, and Rui-Rui Du. Evidence for a topological excitonic insulator in InAs/GaSb bilayers. *Nat. Comm.* **8**, 1971 (2017).

28. L. Du, T. Li, W. Lou, X. Wu, X. Liu, Z. Han, C. Zhang, G. Sullivan, A. Ikhlassi, K. Chang, and R. Du. *Phys. Rev. Lett.* **119**, 056803 (2017).

29. M. V. Weckwerth, J. A. Simmons, N. E. Harff, M. E. Sherwin, M. A. Blount, W. E. Baca, and H. C. Chui, Epoxy bond and stop-etch (EBASE) technique enabling backside processing of (Al)GaAs heterostructures, *Superlattices and Microstructures* **20**, 561 (1996).

30. B. N. Narozhny, A. Levchenko, Coulomb drag, *Rev. Mod. Phys.* **88**, 025003 (2016).

31. In closed-circuit Coulomb drag measurement, an electric current I_1 flowing through one of the layers, known as the "active" layer, induces a current (or, in an open circuit, a voltage V_2) in the other, "passive" layer by means of "mutual friction. By this one typically understands scattering between charge carriers belonging to different layers. The drag resistivity ρ_D in the passive layer is proportional to the interlayer scattering rate $\rho_D \propto \tau_D^{-1}$, and the drive resistivity ρ_{xx} in the active layer can be expressed as Eq. (1).

32. Partial screening effect in electron-hole double layer would occur when the carriers in one layer are tuned to very dilute, thus the selective depletion method (like J. Eisenstein *et al.*, 1990) for an independent-layer contact could not apply to this system. A possible approach to independently contact to hole layer is to metalize InGaSb QW surface like the process in electron layer. However, by etching selectively down to the InGaSb QW, the Fermi level would move upward into the InGaSb band gap, resulting in the failure of the electrical contact to the hole layer.

33. M. J. Yang, C. H. Yang, B. R. Bennett, and B. V. Shanabrook, Evidence of a hybridization gap in "semimetallic" InAs/GaSb systems, *Phys. Rev. Lett.* **78**, 4613 (1997).

34. Yu. Vasilyev, S. Suchalkin, K. von Klitzing, B. Meltser, S. Ivanov, and P. Kopev, Evidence for electron-hole hybridization in cyclotron-resonance spectra of InAs/GaSb

heterostructures, *Phys. Rev. B* **60**, 10636 (1999).

35. Kyoichi Suzuki, Sen Miyashita, and Yoshiro Hirayama, Transport properties in asymmetric InAs/AlSb/GaSb electron-hole hybridized systems. *Phys. Rev. B* **67**, 195319 (2003).

36. C. Nguyen, B. Brar, H. Kroemer, and J. H. English, Surface donor contribution to electron sheet concentrations in not-intentionally doped InAs-AlSb quantum wells. *Appl. Phys. Lett.* **60**, 1854 (1992).

37. G. Tuttle, H. Kroemer, and J. H. English, Electron concentrations and mobilities in AlSb/InAs/AlSb quantum wells. *J. Appl. Phys.* **65**, 5239 (1989).

38. G. Tuttle, H. Kroemer, and J. H. English, Effects of interface layer sequencing on the transport properties of InAs/AlSb quantum wells: Evidence for antisite donors at the InAs/AlSb interface. *J. Appl. Phys.* **67**, 3032 (1990).

39. It can be found that at higher temperatures (*e.g.*, ~19K), more donor states are thermally excited above the potential trap imposed by the disorder, thus resulting in ρ_{xx} independent of V_{BG} before the partial screening takes place.

40. M. Lakrimi, S. Khym, R. J. Nicholas, D. M. Symons, F. M. Peeters, N. J. Mason, and P. J. Walker, Minigaps and novel giant negative magnetoresistance in InAs/GaSb semimetallic superlattices. *Phys. Rev. Lett.* **79**, 3034 (1997).

Figure Captions

FIG. 1. (Color Online) Figure (a) shows a sketch of InAs/InGaSb double layer device. Electrons and holes are confined in InAs and InGaSb QWs respectively. Figure (b) shows eight-band $k \cdot p$ model result of the band structure for InAs/InGaSb double layer. Figure (c) shows schematic view of our device and measurement geometry. The device has a 10nm AlSb middle barrier.

FIG. 2. (Color Online) T=0.3K, ρ_{xx} and corresponding electron density n in the electron layer as a function of V_{TG} for different bottom gate biases stepped in units of 2.5V.

FIG. 3. (Color Online) Figure (a) shows ρ_{xx} as a function of V_{TG} and V_{BG} in zero magnetic field at T = 0.3K. Figure (b), (c) and (d) show V_{BG} dependent ρ_{xx} at V_{TG} = -1.98V, -1.72V and -1V respectively. The corresponding plotted data n in top layer are determined from the small field slope of the Hall resistance.

FIG. 4. (Color Online) Magnetic-field and temperature dependences of ρ_{xx} at V_{TG} =-1.98V. Figure (a). Temperature dependence of ρ_{xx} at zero B. The resistivity signals in the rectangle are highlighted. Figure (b) and (c). T = 0.3K, ρ_{xx} as a function of V_{BG} at different $B_{//}$ and $B_{\perp}$. The $B_{\perp}$-dependent resistivity values of the signals are plotted in the inset of Fig. (c). Circles are experiment data and solid curve is the quadratic fit of the data.
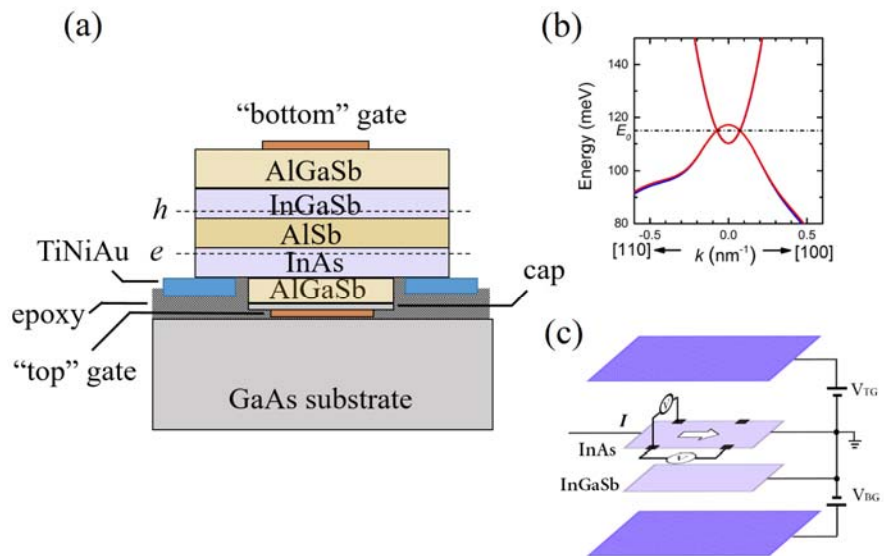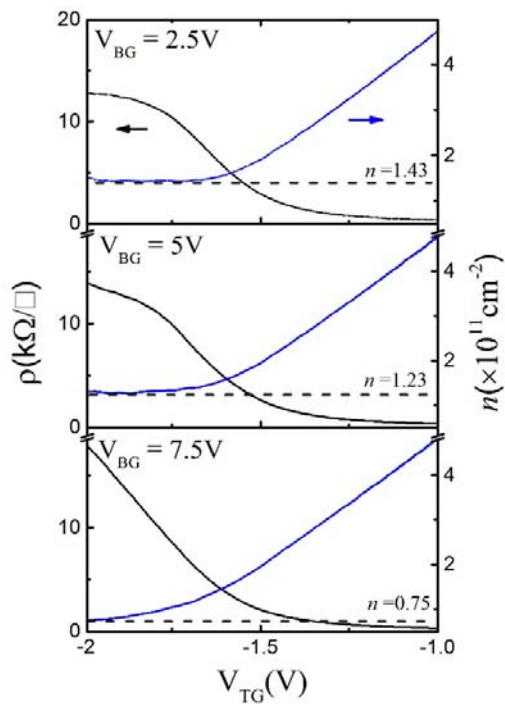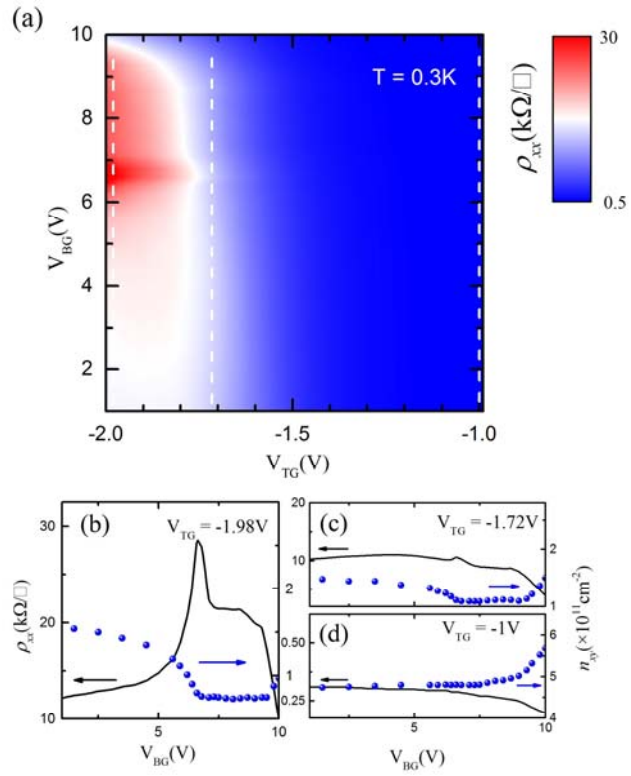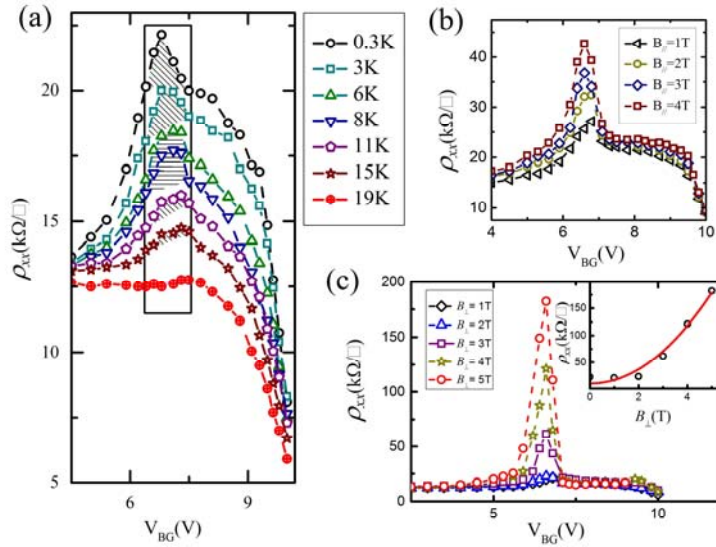
Figure 1

Figure 2

Figure 3

Figure 4